Preprints.org

Article

Not peer-reviewed version

The Solid Solution between NaClO3 and NaBrO3 Revisited

SIMON Roger Florent , Nicolas Couvrat , Christelle Bilot , Sylvain Marinel , Sylvie Malo , Gerard François Coquerel *

Posted Date: 22 June 2023

doi: 10.20944/preprints202306.1610.v1

Keywords: Sodium Chlorate, Sodium Bromate, solid solutions, stable & metastable equilibria, spray-drying

Preprints.org is a free multidiscipline platform providing preprint service that is dedicated to making early versions of research outputs permanently available and citable. Preprints posted at Preprints.org appear in Web of Science, Crossref, Google Scholar, Scilit, Europe PMC.

Copyright: This is an open access article distributed under the Creative Commons Attribution License which permits unrestricted use, distribution, and reproduction in any medium, provided the original work is properly cited.

Preprints (www.preprints.org) | NOT PEER-REVIEWED | Posted: 22 June 2023 doi:10.20944/preprints202306.1610.v1

Disclaimer/Publisher's Note: The statements, opinions, and data contained in all publications are solely those of the individual author(s) and contributor(s) and not of MDPI and/or the editor(s). MDPI and/or the editor(s) disclaim responsibility for any injury to people or property resulting from any ideas, methods, instructions, or products referred to in the content.

Article

The Solid Solution between $NaClO_3$ and $NaBrO_3$ Revisited

Florent SIMON [1], Nicolas COUVRAT [1], Christelle BILOT [2], Sylvain MARINEL [2], Sylvie MALO [2] and Gérard COQUEREL [1,*]

[1] Univ Rouen Normandie, SMS, UR 3233, F-76000 Rouen, France
[2] ENSICAEN, UNICAEN, CNRS, CRISMAT, NORMANDIE UNIV, CAEN 14000, France

Abstract: $NaClO_3$ and $NaBrO_3$ are believed to form a complete solid solution from RT to fusion. The unique solid phase can thus be written: $NaClO_{3\,(1-x)}$-$NaBrO_{3\,(x)}$ with: $0 \leq x \leq 1$. This study shows that at high temperature this statement might be valid. Nevertheless, up to 50°C and probably up to 160°C and even higher temperature, this is not true when the system is in thermodynamic equilibrium. A large miscibility gap exists at room temperature (RT). This gap could be reduced up to a complete disappearance by fast crystallization, for instance by spray-drying. The necessary conditions to access to equilibrium including homochirality are also discussed.

Keywords: Sodium Chlorate; Sodium Bromate; solid solutions; stable & metastable equilibria; spray-drying

1. Introduction

1.1. General concept of solid solutions and motivations for the choice of $NaClO_3$ - $NaBrO_3$ system.

Solid solutions by substitution are often encountered among inorganic and metallic systems as soon as the change between the two species can be simply the replacement of an atom by another atom with a close atomic radius. Often, in such system, the lattice parameters of the solid solution for a given composition follow a Vegard's rule i.e., there is a linear relation between the lattice parameters of the crystalline structure with the concentration of each of the components of the system [1]. However, this empirical law was found not to be the general case, especially for metals [2,3].

Among inorganic solid solutions described in the literature, the $NaClO_3$-$NaBrO_3$ binary system (or $NaClO_3$ – $NaBrO_3$ – H_2O ternary system) has been widely studied. This may be partly due to the high crystallogenic character of the two components and their mixtures. Moreover, $NaClO_3$, $NaBrO_3$ and $NaClO_{3(x)}BrO_{3(1-x)}$ intermediate compositions have low melting points [5] and high (ClO_3-rich) to medium (BrO_3-rich) solubilities in water [6,7]. $NaClO_3$ has a melting point of 262°C and a solubility in water of 790g.l^{-1}. $NaBrO_3$ has a melting point of 347°C and a solubility in water of 275g.l^{-1}.

1.2. Crysal structure of $NaClO_3$ and $NaBrO_3$ pure compounds.

Sodium chlorate ($NaClO_3$, MW=106.44g.mol^{-1}, T_{fus} = 248°C) and sodium bromate ($NaBrO_3$, MW = 150.89g.mol^{-1}, T_{fus} = 381°C) have isomorphous crystal structures that were formerly investigated by Dickinson in 1921 [8]. Both halates crystallize in the chiral space group $P2_13$ (tertartohedral group in the cubic system), with crystalligraphic parameters a = 6.57584(5) and a = 6.70717(10) Angströms, respectively at RT [9]. The space group $P2_13$ is chiral thus, noncentrosymmetric in adequation with the property to exhibit second order nonlinear optical phenomena [10,11] (Savage, 1962; Simon, 1968).

1.3. Chirality and deracemization.

$NaClO_3$ and $NaBrO_3$ belong to achiral molecules that exhibit supramolecular chirality in the solid state [12]. It was also found that optically dextro (D) rotatory $NaClO_3$ has the opposite configuration than the optically dextro (D) rotatory $NaBrO_3$, or, in other words $(NaClO_3)_D$ has the same structural configuration as $(NaBrO_3)_L$ [13–15]. Thus, the $(NaClO_3)_L$/$(NaClO_3)_D$/$(NaBrO_3)_L$/$(NaBrO_3)_D$ system is quaternary, when the solid phases are considered.

Deracemization (conversion of a racemic mixture to a pure enantiomer) in $NaClO_3$ supersaturated solution was first observed by Kipping and Pope [16] (Kipping, 1898). Later on further experiments were conducted by Kondepudi *et. al.* on $NaClO_3$ [17]. They observed that from a supersaturated solution under stirring, the resulting solid crystals were of the same chiral configuration. When the solution is stirred, fragments of a single configuration are dispersed in the media promoting their growth and inhibiting primary nucleation which normally generate an equal proportion of nuclei with opposite chiral configuration. Their work relies on the general conception of sensitivity of nonequilibrium

© 2023 by the author(s). Distributed under a Creative Commons CC BY license.

Preprints (www.preprints.org) | NOT PEER-REVIEWED | Posted: 22 June 2023 doi:10.20944/preprints202306.1610.v1

systems [18–20]. Buhse *et. al.* reported an interesting observation: deracemization can occur in $NaClO_3$ supersaturated solutions in which a $NaBrO_3$ crystal has been inoculated. $NaBrO_3$ acts as a template of crystallization for only one of the $NaClO_3$ chiral configuration (as $NaClO_3$ and $NaBrO_3$ are isomorphous) [21].

In 2005, Viedma reported later that deracemization could also occur in suspension of $NaClO_3$ [22]. He showed that continuous attrition on a suspension of sodium chlorate leads to the switch from a racemic population of lefthanded and right-handed crystals to a homochiral population of crystals. The possibility of a mechanism governed by reincorporation of clusters that are below the critical size of equilibrium is discussed. In 2011, Viedma and Cintas reported the use of dissolution-crystallization cycles (in boiling solutions) as an additional mechanism for the deracemization of $NaClO_3$ [25]. The same phenomenon has been observed with different sources of energy crossing the suspension: Ultrasound, pressurization, and temperature cycling [23]. Actually, for the latter, there is no need to form large temperature swings, continuous small oscillations in the temperature of the suspension lead to an irreversible evolution towards homochirality. Moreover, those different ways of deracemization could be coupled with agonist effects [24]. Viedma et al. found that large aggregates formed by several crystals with only one chiral configuration could be obtained [26]. With this method, aggregates can be simply separated manually under a polarized microscope as soon as their size was about 5-10mm. In 2020, Schindler *et. al.* found that the use of dithionate impurity, also known to be a habit modifier for $NaClO_3$ (see next paragraph) could, however, strongly delay this mechanism [27].

Therefore, equilibrium in that system will impose simultaneously: the regular conditions for thermodynamic equilibrium (chemical equilibrium, thermal equilibrium, no segregation and a mechanical equilibrium) and homochirality.

1.4. Crystal growth of $NaClO_3$ and $NaBrO_3$ crystals in the presence of impurities.

Some decades ago, the general concept of crystal growth in the presence of impurities has attracted much attention. Explanation of anomalous optical phenomena, crystal habit modification and overall crystal symmetry breaking, including systems of solid solutions of both inorganic and organic materials were reported in the literature [28–36]. Cases of habit modifications for $NaClO_3$ crystals have been reported since the 19th Century (see discussions in ref. [7,41]).

In particular, the effect of $Na_2S_2O_6$ impurities was widely studied in the literature. Habit modification by dithionate impurity was first reported in 1930 to modify the habit of $NaClO_3$ crystals into a tetrahedral morphology [37].

In the early 90's Ristic *et. al.* studied the growth kinetics and morphology of $NaClO_3$ crystals from the solution in the presence of dithionate impurities [38,39]. They found that the cubic morphology easily switches towards a tetrahedral morphology as soon as a sufficient amount of dithionate impurities was added to the mixture (210ppm). This analysis was rationalized through the geometry of $(ClO_3)^-$ ion being similar to that of one of the $(SO_3)^-$ subgroups of the $S_2O_6^{2-}$ ion on these specific tetrahedral faces, inhibiting the growth of these faces. Recently, Lan *et. al.* investigated deeply this phenomenon to validate a proposed model based on the nature of twinning (observed in $NaClO_3$ crystals) inducing by dithionate impurities [40]. They found notably that at higher dithionate impurities level (1000ppm), twinned crystals can be formed with the particularity that the counter chiral configuration is produced at the twin interface occupied by dithionate impurities. This was due to the ionic structure of $S_2O_6^{2-}$ which consists in two SO_3^- moieties oppositely orientated. This work shows that if a crystal of a single chiral configuration can be produced by deracemization, the presence of dithionate impurities induces on the contrary that aggregates (twin crystals by inversion) are formed of crystalline domains of both chiral configurations.

Interestingly, BrO_3^- ion has been reported to be a habit modifier of $NaClO_3$ (see discussions in refs. [41,42]) and to induce overall symmetry breaking for a wide range of $NaClO_{3(x)}BrO_{3(1-x)}$ intermediate compositions.

1.5. $NaClO_{3(x)}BrO_{3(1-x)}$ mixed crystals: kinetic ordering and deviation from ideal cubic structure.

In 1984, Raja *et. al.* [43] analyzed a crystal with $Na(ClO_3)_{0.7}(BrO_3)_{0.3}$ composition and found that it crystallizes, also, in the cubic $P2_13$ space group, confirming the existence of the solid solution. Nevertheless, many other works indicated different results. Since the 19th century, polarized optical observations on $NaClO_{3(x)}BrO_{3(1-x)}$ solid solution crystals revealed birefringence that is physically not allowed in isotropic cubic structures [7,41,44]. The authors found that apparent single crystals exhibited sectors of different compositions (in both constituents of the solid solution) reducing the overall symmetry of these crystals to the monoclinic $P2_1$ or triclinic $P1$ space groups due to kinetic ordering of atoms during crystallization by water evaporation. Authors of the same research group also indicated a potential segregation of BrO_3^- and ClO_3^- microscale domains within an apparent 'single' crystal through the alternation of dextro- and levorotary domains [42]. A complete study of the $NaClO_{3(x)}BrO_{3(1-x)}$ system was also recently carried out by Su et. al. [45]. Crystals of the solid solution between 14 to 81 wt. % NaBrO3 were found to be of worse optical quality i.e., opaque with cracks contrary to crystals obtained outside this range of composition. For these compositions a very weak diffraction

Preprints (www.preprints.org) | NOT PEER-REVIEWED | Posted: 22 June 2023 doi:10.20944/preprints202306.1610.v1

peak at 13.3° 2θ was found and could be indexed as the (100) peak, forbidden for the $P2_13$ space group (h00; h = 2n), indicating a slight deviation from an ideal cubic structure.
Nevertheless, it was reported that annealing close to the melting temperature leads to a homogenization of the crystals and hence to a return to the $P2_13$ crystal structure [42,45,46]. It was not reported whether the $NaClO_{3(x)}BrO_{3(1-x)}$ solid solution crystals return to an equilibrium state or if a transition towards the cubic structure only possible at higher temperature could remain in a metastable state at room temperature.

1.6. Heterogeneous equilibria.

The first study of the $NaClO_3$ - $NaBrO_3$ system was performed in 1939 by Swenson and Ricci [6], regardless the chirality. They published two isothermal studies of the ternary system $NaClO_3$ - $NaBrO_3$ – H_2O at 25°C and 50°C (Figure 1, a & c). They showed that there might be a complete solid solution between the two components at 50°C (Figure 1, d), but the possible existence of two solid solutions at 25°C was envisaged (Figure 1, b). Indeed, careful examinations of (i) the solubility curve versus composition and (ii) the tie lines in this isotherm at 25°C reveal an odd behavior. In this work the authors suggested that the solid solution was apparently discontinuous. The solubility curve appeared to be divided in three parts corresponding to the following solid phases: (i) solid solution very close to pure $NaBrO_3$, (ii) a bromate solid solution containing few ppm to 5-10% of chlorate, and (iii) a chlorate solid solution containing up to 60-65% chlorate solid solution. Another authors' suggestion was that this solid solution was continuous but with a marked tendency toward the formation of an isothermal invariant point.

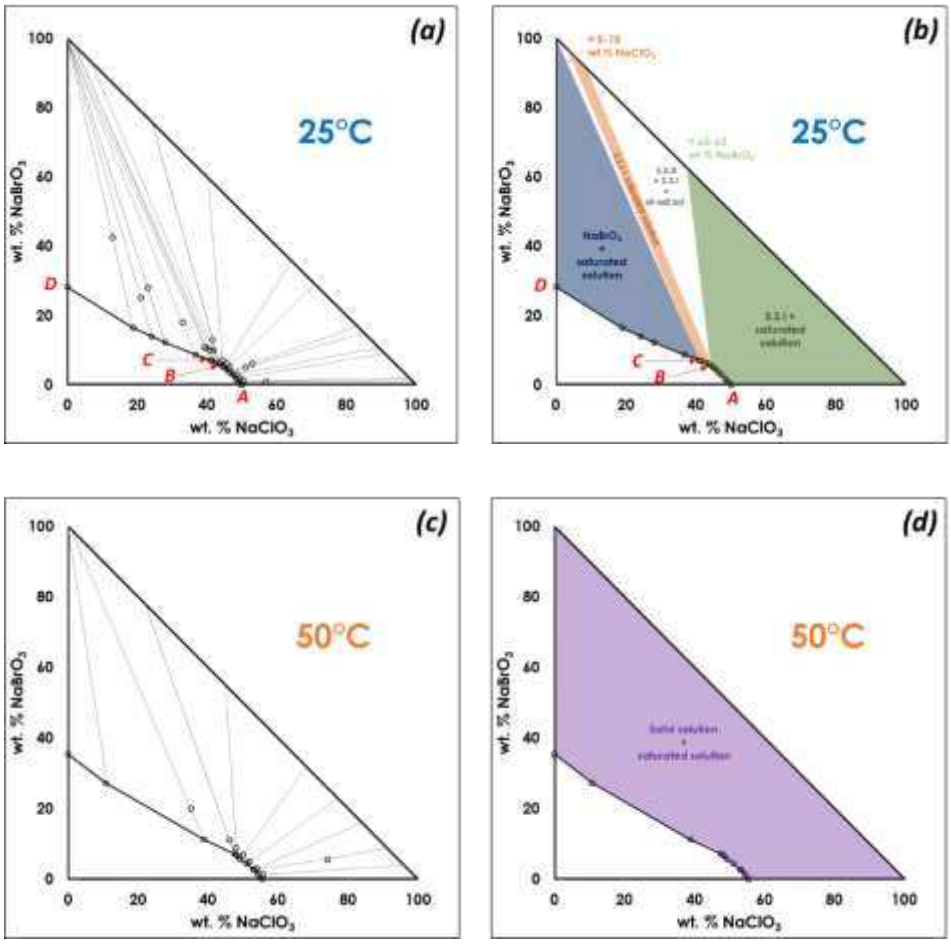

Figure 1. (a)(c) Ternary isothermal sections at 25°C and 50°C proposed by Swenson and Ricci (adapted from ref. (Swenson, 1939)) Note: No XRD data were collected during this work, the recovered solid compositions were determined by titration, so the interpretations of the data can be manifold. (b) Swenson and Ricci's proposal for biphasic domains in the ternary isotherm at 25°C. At this temperature and to be in accordance with Gibbs phase rule, those three biphasic domains need to be interlaced by triphasic domains (triangular white domains). The three regions are represented with different colors. The green domain encompasses, by far, the largest part of the two-phase region from 0% bromate (100% chlorate) to ca. 60-65 wt.% $NaBrO_3$ in the solid phase and from A to B for the corresponding saturated solution. The rather thin region colored in grey, corresponds to a possible ordered domain ranging from 90-95% to almost 100% bromate in the solid phase and from B to C for the corresponding saturated solution. The last region

Preprints (www.preprints.org) | NOT PEER-REVIEWED | Posted: 22 June 2023 doi:10.20944/preprints202306.1610.v1

colored in blue behaves like a pure component; the tie lines are likely to converge to nearly pure sodium bromate and the corresponding saturated solution ranging from C to D. (d) Swenson and Ricci's proposal for equilibria at 50°C showing a continuous solid solution.

1.7. Summary of the literature review and aim of that study

This literature review emphasizes the complex crystallization behavior by water evaporation for the $NaClO_3$ - $NaBrO_3$ system, especially when the $NaClO_{3(x)}BrO_{3(1-x)}$ compositions are far from the respective pure phases. The problem is that crystallization is most often kinetically driven, both by the ability of ClO_3^-/BrO_3^- ions ordering as well as chirality ordering. Notably, both phenomena have been observed within an apparent well shaped single crystal.

The question whether the $NaClO_{3(x)}BrO_{3(1-x)}$ mixed crystals belongs to a complete solution at room temperature (*e.g.*, 25°C) is finally still open, the reason might be that equilibrium seems to be difficult to reach.

Before examining the system regarding the chirality and deracemization of mixed compositions, it appeared necessary to clarify the existence of heterogeneous equilibria between these two components.

2. Material and methods

2.1. Commercial material

Sodium chlorate was purchased from Alfa Aesar with purity of 99%. Sodium bromate was purchased from Merck with purity of 99%.

2.2. Crystallization by solvent evaporation

$NaClO_3$ and $NaBrO_3$ commercial powders were dissolved in water (40mg/mL) to make undersaturated solutions of different $NaClO_3$/$NaBrO_3$ ratios. The whole solutions were transferred to individual opened large crystallization beakers for evaporation at RT or in a temperature regulated ventilated oven. The crystals were collected at the end of evaporation in order to recover the same composition in $NaClO_3$ and $NaBrO_3$ that have been formerly introduced for the preparation of the samples. For some experiments at elevated temperatures, crystallizations were performed in opened vials under stirring.

2.3. Crystallization by spray-drying

The spray dryer used in this study is a Büchi B290 (conventional laboratory dryer designed with a co-current configuration). Compressed gas used is nitrogen and feeding solutions were aqueous solutions. The laboratory-scale spray dryer was equipped with a nozzle 0,7 mm in diameter (Tip = 0.7mm; Cap = 1.4mm).
Several mixtures were dissolved in water, with the following parameters (Table 1):

Table 1. Spray-drying parameters for two sets of experiments.

Parameters	Protocol 1	Protocol 2
Concentration of the $NaClO_{3(1-x)}$-$NaBrO_{3(x)}$ aqueous solutions	2g/150mL water	6g/50mL water
Inlet temperature of the drying nitrogen	220°C	220°C
Feed flow rate (peristaltic pump)	360mL/h	300mL/h
Temperature of the feed solution	Room temperature	Ca. 60°C
Atomizing airflow rate	473L/h	500L/h
Aspiration	40m³/h	40m³/h
Location of the powder at the end of the process	Mainly in the bowl collector	In the drying chamber, cyclone and bowl collector

2.4. XRPD

XRPD patterns were obtained either with a Da Vinci D8 Bruker X-ray diffractometer with a Bragg-Brentano geometry (θ//θ)or a D8 diffractometer (Bruker, Germany) equipped with a modified goniometer of reverse-geometry (-θ/-θ) [47](Coquerel, 2015). For both instruments, the incident X-ray beam consisted of the Cu Kα (λ = 1.5418 Å) with a tube voltage and amperage set at 40 kV and 40 mA respectively. The diffraction patterns were collected with a LynxEye® linear detector (Bruker, Germany). Routine XRPD analyses were performed with a step of 0.04° (2θ), and a 12 s per step counting time from 3° to 30° (2θ). The system is monitored with DiffracPlus XRD commander software version 2.6.1. Data were processed with DIFFRAC.EVA software release 2018 (version 4.3.0.1).

Preprints (www.preprints.org) | NOT PEER-REVIEWED | Posted: 22 June 2023 doi:10.20944/preprints202306.1610.v1

2.5. TR-XRPD

Solid crystalline phases were analyzed by means of X-ray powder diffraction (XRPD) on D8 advance series II diffractometer (Bruker analytic X-ray Systems, Germany). The instrument is equipped with an X-ray tube containing a copper anticathode, (40 kV, 40 mA) and a LynxEye® linear detector for every XRD scan, the step size was fixed at 0.04° with a counting time of 0.5s/step over an angular range 10°- 40° (2-theta). Temperature was controlled and monitored using a TTK 450 heating stage (Anton Paar GmbH, Austria). Data were processed with Eva software version using DIFFRAC.EVA software release 2018 (version 4.3.0.1).

2.6. DSC

DSC experiments in the temperature range 0 °C to 400 °C were performed using a Netzsch DSC 204 F1 apparatus equipped with an intracooler. Each DSC run was performed with ca. 5-15 mg of a powdered sample in aluminum pans with pierced lids at 2 or 5 K/min heating rates. The atmosphere of the analyses was regulated by a helium flux (40 mL/min). Onset (respectively endset) temperatures are calculated from the intersection between the baseline and the slope of the first (respectively last) part of the endotherm.

2.7. SEM

Scanning electron microscopy (SEM) pictures were obtained with a JEOL JCM-5000 NeoScope instrument (secondary scattering electron) at an accelerated voltage of 10kV. Samples were stuck on a SEM stub with gloss carbon and coated with gold to reduce electric charges induced during analysis with a NeoCoater MP-19020NCTR.

2.8. SEM-EDX

Scanning Electron Microscopy (JEOL JSM 7200F) coupled with Energy Dispersive X-Ray spectrometer (EDX XFLASH 6160 from Bruker) was used to collect images and for quantitative chemical analysis. EDS spectra were collected under a voltage of 10 kV with a working distance of 10 mm. Although no conductive coatings were deposited, the experimental conditions were satisfactory to record BSE (Back Scattered Electrons) images and for X-ray mapping experiments.

2.9. Optical microscope

Polarized Optical Microscopy (POM) observation was conducted by using a Nikon SMZ-10A microscope (Nikon imaging Ltd.) coupled to CCD-camera connected to a computer. Data processing was run by using LEICA Microsystems Application Suite X software.

3. Results and discussion

A. Confirmation of kinetic ordering through classical (slow) water-evaporation crystallization process evidence of a miscibility gap at 20°C.

In order to confirm the existence of a complete solid solution, or by contrast, the presence of two limiting solid solutions with a miscibility gap, several 50wt.% $NaClO_3$/$NaBrO_3$ mixtures in aqueous solutions were dissolved and left under stagnant conditions to fully evaporate at: 20°C, 50°C, 80°C, 100°C, 120°C and 150°C. In all cases two closely related XRPRD patterns were obtained (Figure 2). Despite the isomorphous character of $NaClO_3$ and $NaBrO_3$ single phases, the XRPD patterns of the 50wt.% powder sample obtained after evaporation at room temperature clearly indicated a miscibility gap in the solid state (Figure 2, a). A careful examination of the peaks of the powder samples crystallized at RT revealed that the two solid phases obtained are not constituted by a physical mixture of pure $NaClO_3$ and pure $NaBrO_3$, but rather constituted by a physical mixture of two solid solutions with limiting domain of existence. Thus, a large miscibility gap exists from ca. 20wt.% $NaBrO_3$ to ca. 70wt.% $NaBrO_3$. This miscibility gap was confirmed to exist (at least) up to 160°C from the evaporation experiments conducted at elevated temperatures (Figure 2, b).

Preprints (www.preprints.org) | NOT PEER-REVIEWED | Posted: 22 June 2023 doi:10.20944/preprints202306.1610.v1

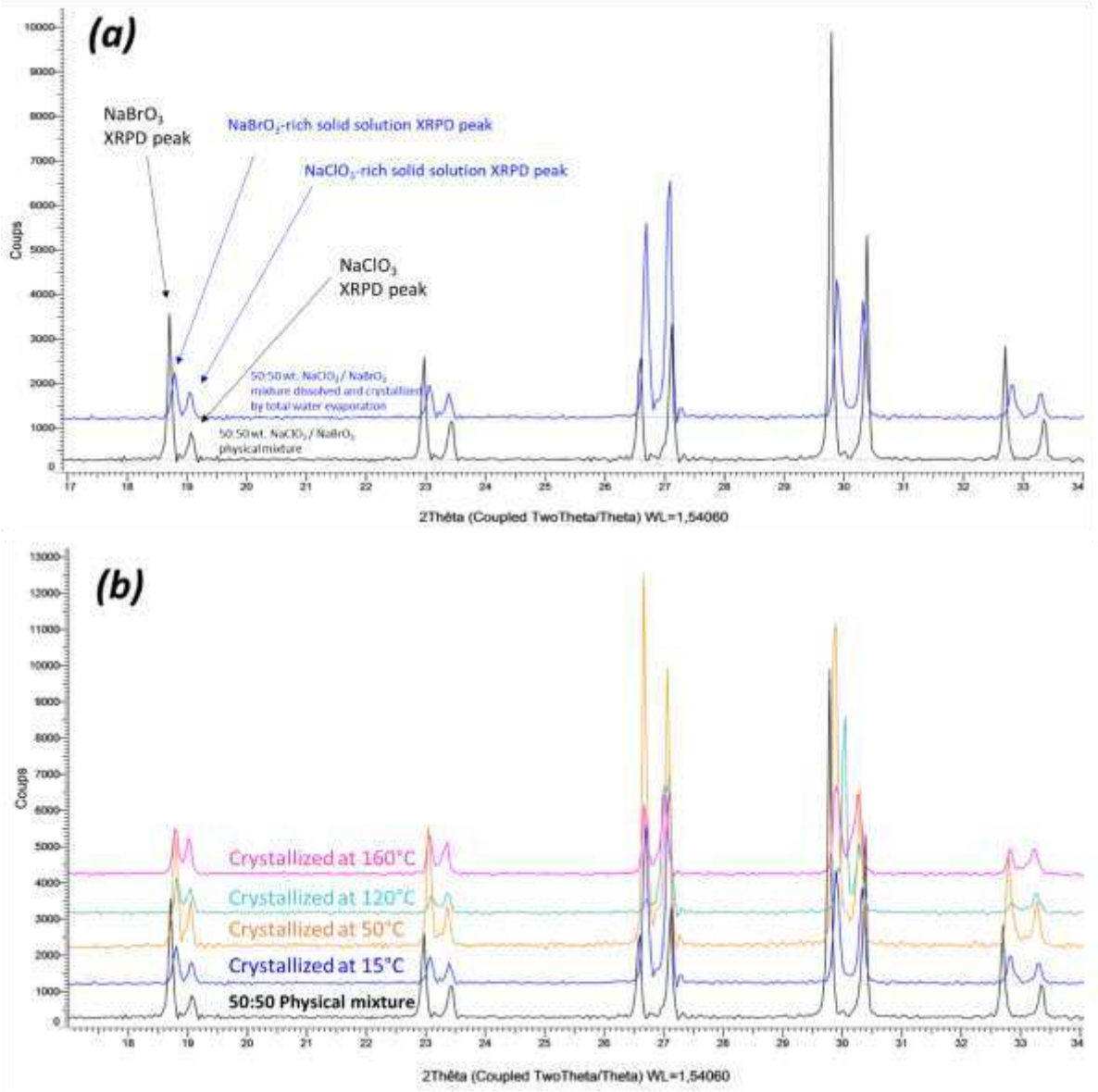

Figure 2. (a) XRPD pattern of powder sample (crystallized by slow evaporation under stirring from 50wt.% $NaClO_3$/$NaBrO_3$ mixtures in aqueous solution) in comparison with pure $NaClO_3$ and $NaBrO_3$ commercial samples (physical mùixture). Based on the peak position, a rough estimation of the limiting composition of $NaClO_3$-rich and $NaBrO_3$-rich solid solution indicated 20wt.% and 70wt.% in $NaBrO_3$, respectively. Thus two partial solid solutions exist: one $NaClO_3$-rich solid solution (hereafter labelled S.S.I) ranging from 0wt.% to 20wt.% $NaBrO_3$, and one $NaBrO_3$-rich solid solution (hereafter labelled as S.S.II) ranging from 70wt.% to 100wt.% $NaBrO_3$. (b) XRPD patterns of powder samples crystallized by slow evaporation from 50wt.% $NaClO_3$/$NaBrO_3$ mixtures in aqueous solution at different temperature: RT, 15°C, 50°C, 120°C, and 160°C) confirmed that the miscibility gap is still present at elevated temperature.

Crystallization pathway, from undersaturated solution towards total evaporation, was investigated on a 50wt.% $NaClO_3$/$NaBrO_3$ mixture dissolved in water (Figure 3). During evaporation, several single particles were withdrawn at different times to investigate the solid phase. Results confirmed the solid-solid demixion (S.S.I + S.S.II + di-saturated saturated solution) during the last crystallization episodes.

Preprints (www.preprints.org) | NOT PEER-REVIEWED | Posted: 22 June 2023 doi:10.20944/preprints202306.1610.v1

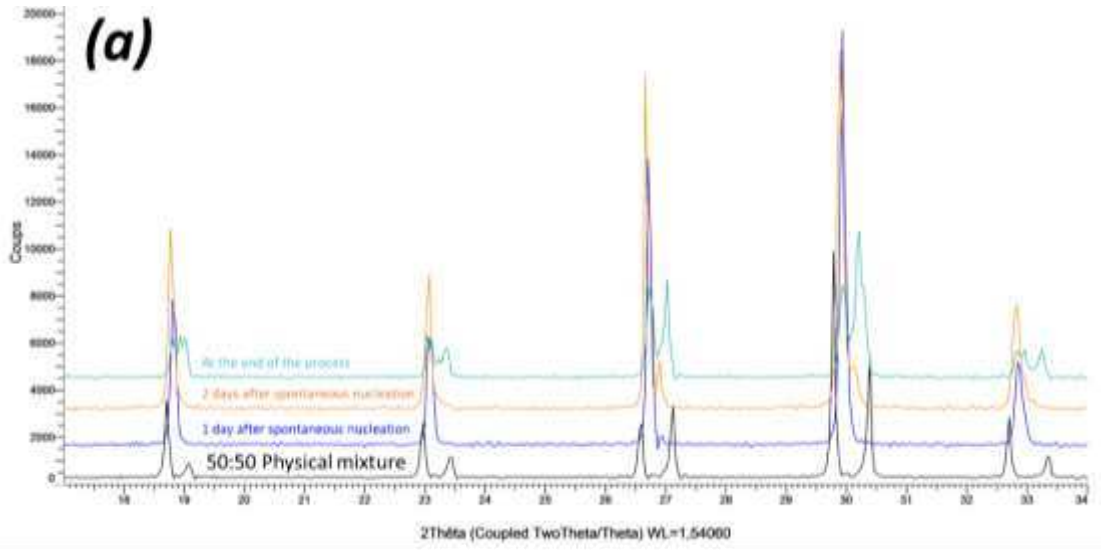

Figure 3. XRPD patterns of single particles withdrawn from an open crystallizer at different times during water evaporation: (black XRPD pattern): 50:50 $NaClO_3$/$NaBrO_3$ physical mixture (reference); (blue XRPD pattern) particle withdrawn after 1 day after spontaneous nucleation; (orange XRPD pattern) after two days after spontaneous nucleation; (green XRPD pattern) at the end of the process (total evaporation). Only one particle was withdrawn at a time so the overall composition of the system remained unchanged.

Large crystals were obtained by water evaporation at 20°C and submitted to a polarized microscopic inspection (Polarized Optical Microscopy: POM hereafter) (Figure 4) and SEM-EDX analysis (Figure 5).
POM pictures reveal that what appear as single particles are actually a patchwork of domains of different sizes and geometries. POM reveals also that the chirality of those domains can differ even within the same crystallographic sector (Figure 4).

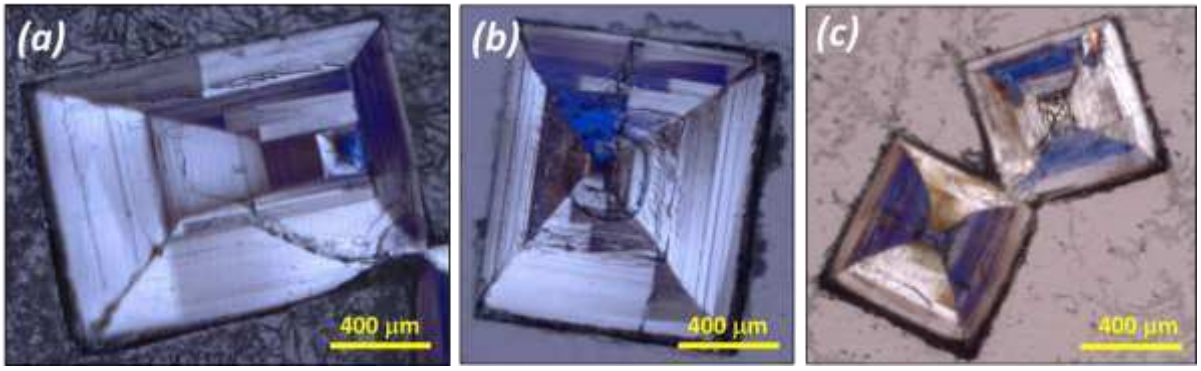

Figure 4. Polarized-light optical microscopy (POM) of selected $NaClO_{3(x)}BrO_{3(1-x)}$ mixed crystals grown by complete evaporation at 20°C from 50wt.% $NaClO_3$/$NaBrO_3$ mixtures in aqueous solution. (a), (b) and (c) show apparent single crystals revealing domains of different handedness. Hopper defects (concave crystals) were often found, because crystal edges and corners grow faster than surfaces for large crystals grown at high supersaturation without stirring.

EDX analysis on two spots belonging to two different domains reveal an almost inverted composition between Cl and Br (8.6 Cl & 30.5 Br atom % for spot 1) and (24.8 Cl and 6.2 Br atom % for spot 2). It can be surmised that those particles are in fact composed of four different domains: supramolecular left and right domains enriched in Bromate and supramolecular left and right domain enriched in chlorate. Due to the poor solubility of the bromate compared to the chlorate it is logical that the center of the particle is enriched in bromate.

Preprints (www.preprints.org) | NOT PEER-REVIEWED | Posted: 22 June 2023 doi:10.20944/preprints202306.1610.v1

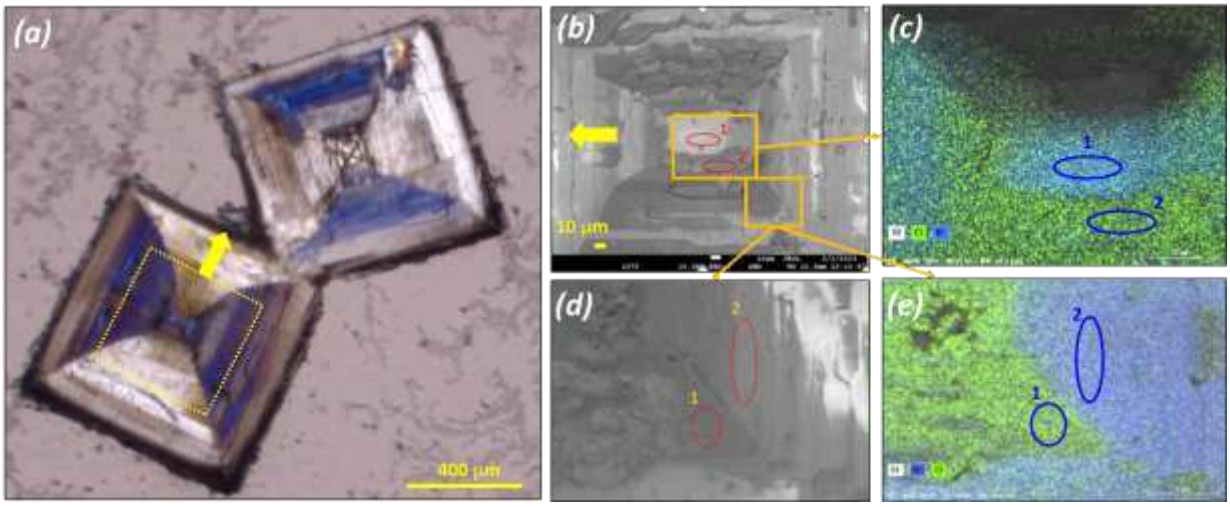

Figure 5. Mapping by EDX of a large particle obtained by slow aqueous evaporation at room temperature from a 50wt.% NaClO3/NaBrO3. Mixture. (a)Polarized Optical Microscopy POM pictures showing the particle. (b) and (d) SEM pictures of selected area of the selected particle. (c) and (e) corresponding composition mapping by EDX showing different concentration of Cl and Br atoms depending on the selected zone on the particle: (c) zone 1: molar Br ratio = 30.5/(30.5+8.6) = 78%; zone 2: molar Br ratio = 20%; (e) zone 1: molar Br ratio = 21%; zone 2: molar Br ratio = 81%.

From the above data we can conclude that, when the thermodynamic equilibrium is attained, sodium chlorate and sodium bromate do not form a complete solid solution from room temperature up to 160°C, but rather two partial solid solutions. It is likely that the miscibility gap in the solid-state extents to much higher temperatures

In order to see if the miscibility gap in the solid state intersects the solid liquid equilibria, temperature, resolved X-ray powder diffraction experiments (TR-XRPD) were run for the 50% (mass) composition (Figure 6). Several heating ramps up to 250°C were used on the same sample. These thermal treatments with annealing for 11 h at high temperature, were interspersed with a flattening of the powder to avoid the retreat effect of sintering.

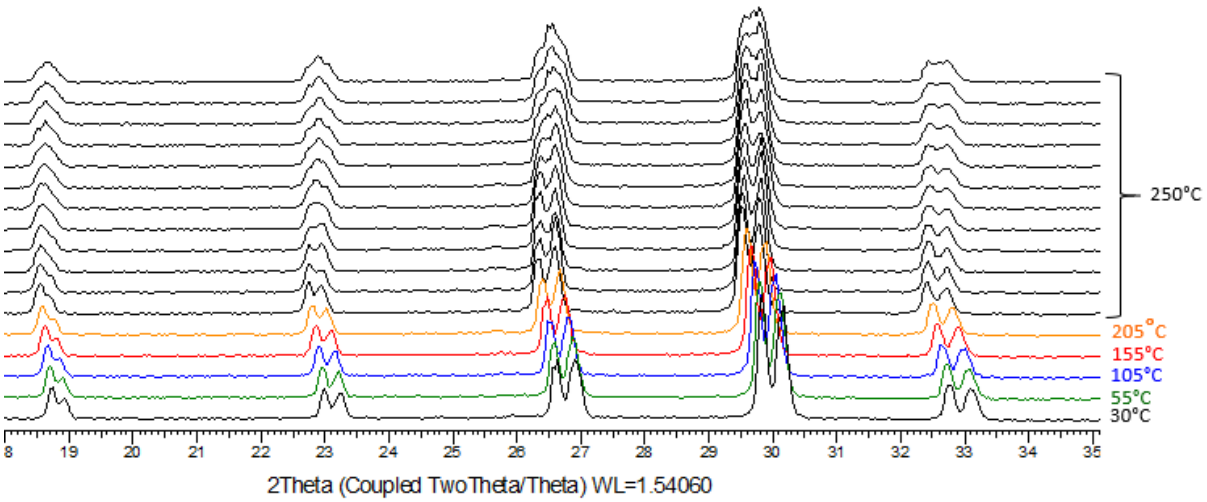

Figure 6. TR-XRPD of a 50% Mass Composition from 85°C to 250°C, annealing of the 11 last patterns (11h) at 250°C.

Figure 6 shows the third analysis on heating. A careful inspection of the evolution of the diffraction peaks versus temperature shows that the two patterns, related to the presence of a $NaClO_3$-rich and a $NaBrO_3$-rich solid solution, tend to collapse into a single one. Even if the annealing temperature was close to that of the solidus (see experimental points (filled circles) on Figure 7), a genuine complete merge of the two patterns is not observed. Longer annealings have shown the beginning of decomposition and therefore could not be prolonged, furthermore. The opposite supramolecular chirality of the particle may not help the sintering. Therefore, this work leads to two hypotheses shown Figure 7 (a) and Figure 7 (b).

Preprints (www.preprints.org) | NOT PEER-REVIEWED | Posted: 22 June 2023 doi:10.20944/preprints202306.1610.v1

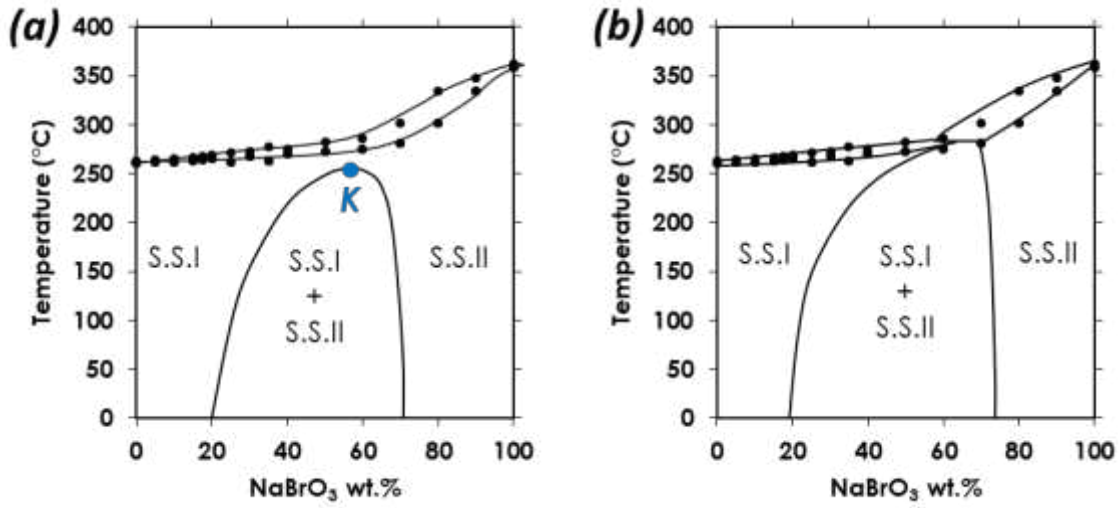

Figure 7. (a) Putative homochiral binary phase diagram between $NaClO_3$ and $NaBrO_3$ showing a stable miscibility gap up to a critical point (K), above which a long period of diffusion time could succeed in mixing the two components in the full range of composition (i.e., from 0 to 100% $NaBrO_3$). Note that homochirality is supposed to appear to give left-handed or right-handed crystals only. (b) Putative homochiral binary phase diagram between $NaClO_3$ and $NaBrO_3$ showing a stable miscibility gap that does not close up at elevated temperature but intersects the liquid-solid equilibria, implying a three-phase invariant (peritectic transition). Note: for both (a) and (b), filled circles corresponds to experimental points determined by DSC (present work).

B. Crystallization of $NaClO_3$/$NaBrO_3$ mixtures by spray-drying. Evidence of a metastable complete solid solution.

Literature shows that homogeneity could be an issue in the preparation of samples with different compositions, therefore mixtures $NaClO_{3(x)}BrO_{3(1-x)}$ $0 \leq x \leq 1$ have been prepared by spray-drying according to *Protocol 1*.

It can be surmised that in every droplet a Kondepudi-like crystallization occurs. Accordingly, on drying, every droplet should give homochiral particles unless there is a bias in the nucleation process due to the presence of an active chiral impurity. The global result should be statistical nucleation of right-handed and left-handed particles, in other words: a racemic mixture. A recent article details the link between size and homochirality [48].

The obtained particles exhibit morphologies that are more isomorphous than crystallization from stagnant solution for which the habitus are flattened with characteristic defects (Figure 4).

Preprints (www.preprints.org) | NOT PEER-REVIEWED | Posted: 22 June 2023 doi:10.20944/preprints202306.1610.v1

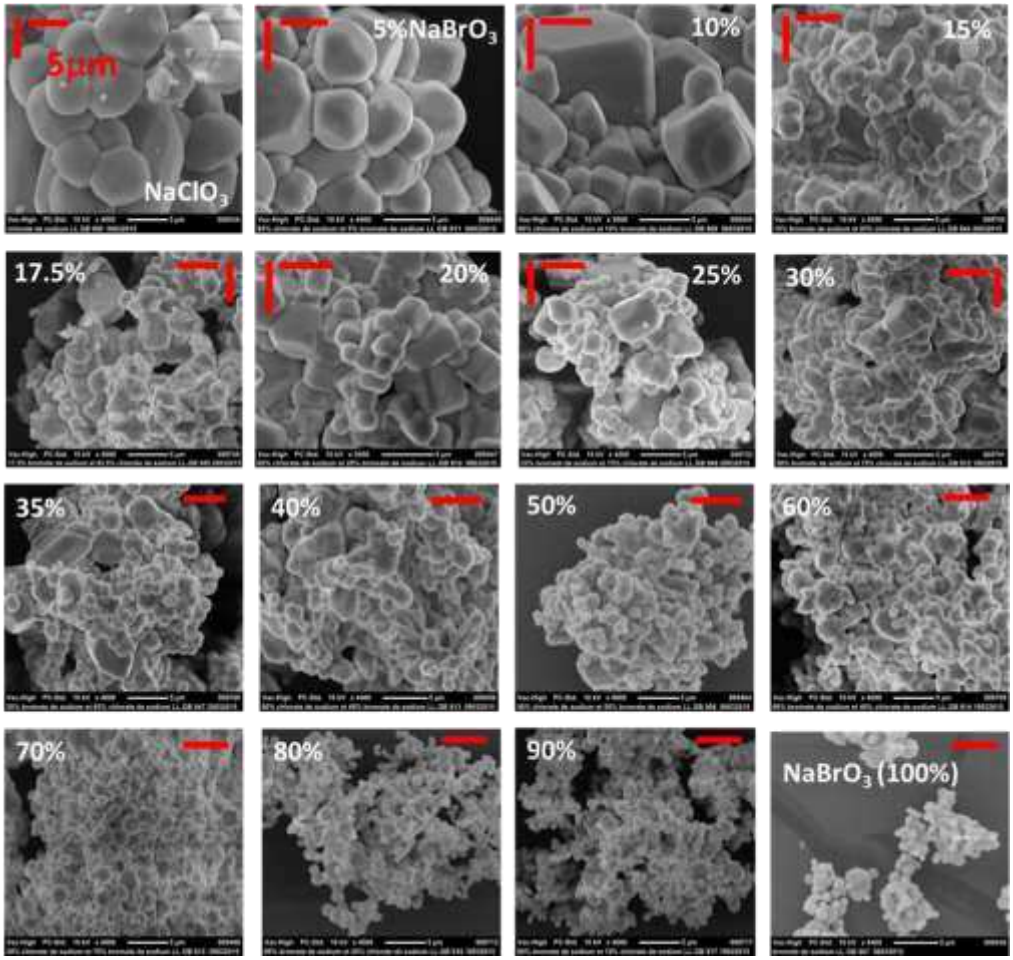

Figure 8. SEM pictures--with the same magnification- of spray-dried samples obtained by using Protocol 1 from different initial compositions (ranging from 0% $NaBrO_3$ (100% $NaClO_3$) to 100% $NaBrO_3$ (0% $NaClO_3$)). As $NaBrO_3$ is less soluble than $NaClO_3$, particles were found to be smaller. .

XRPD patterns on fresh spray-dried samples recorded at room temperature are displayed on Figure 9. Contrary to powder samples obtained by slow water evaporation, the inlet shows the shift of the X-Ray diffraction peak versus composition in the full range $0 \leq x \leq 1$. Furthermore,

Preprints (www.preprints.org) | NOT PEER-REVIEWED | Posted: 22 June 2023 doi:10.20944/preprints202306.1610.v1

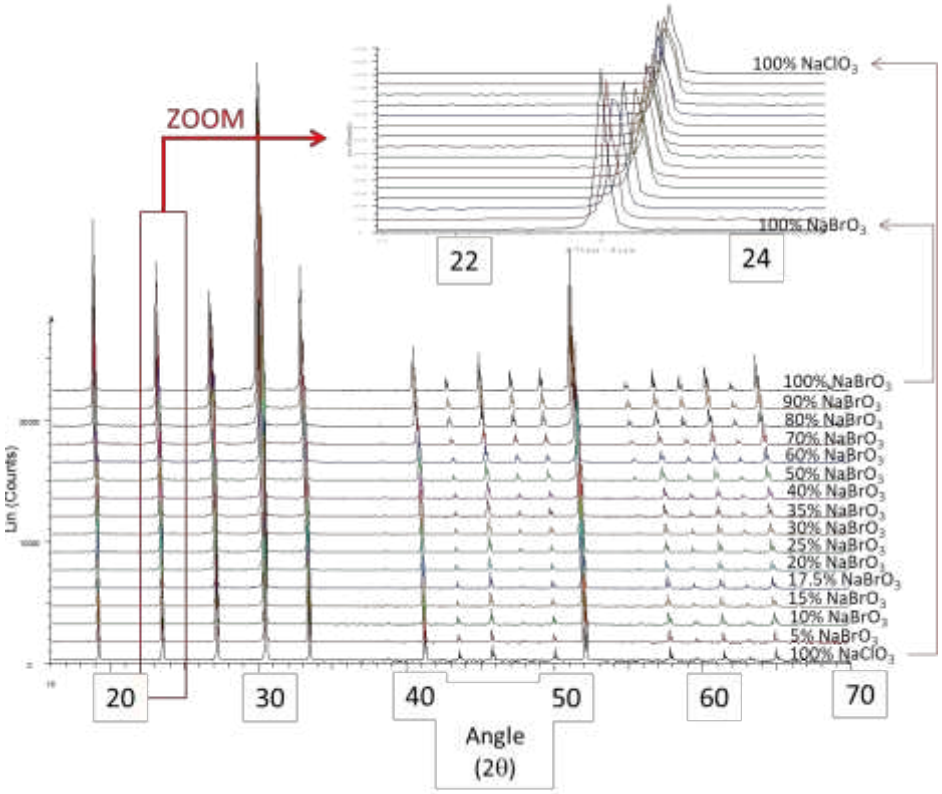

Figure 9. XRPD pattern versus composition of $NaClO_{3(x)}BrO_{3(1-x}$ (mass fraction) prepared by spray-drying -protocol 1- The inlet is a zoom on the second peak at ca. 23 ° (2θ scale Cu Kα.).

The evolution of the cubic unit-cell parameter at RT as function of the mol fraction of $NaBrO_3$ is represented on Figure 10. Although the maximum difference between $NaClO_3$ and $NaBrO_3$ lattice parameter is only 1.92%, a discontinuity of the Vegard law is observable, that could reflect the metastable character of the solid solution. In the composition region ranging from ca. 20wt.% to 70wt.% (that is, by the way, closely similar to the limiting compositions of $NaClO_3$-rich and $NaBrO_3$-rich solid solution observed in the case of crystallization by slow solvent-evaporation), the density of the solid phases appears to be slightly higher than the two normal trends.

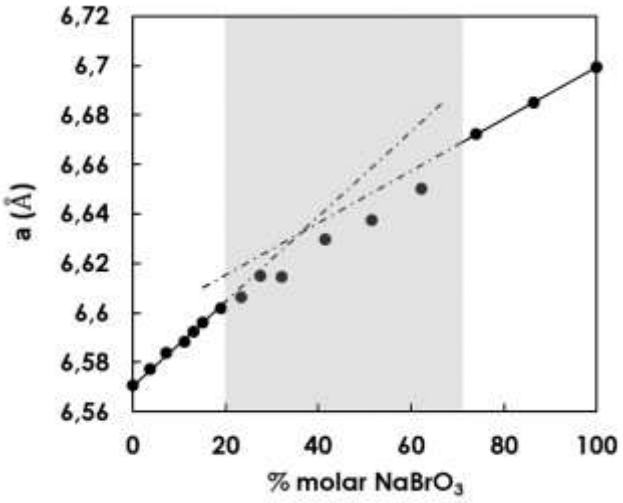

Figure 10. Crystallographic parameter **a** of $NaClO_{3(x)}BrO_{3(1-x}$ (molar fraction) prepared by spray-drying -using protocol 1 (precise values are reported in Table SI-1). A discontinuity of the Vegard law seems to be present for compositions ranging from ca. 20% to ca. 70% NaBrO3, for which the cubic cell parameter seems to be slightly lower than the mean of parameters limiting the partial solid solutions.

Preprints (www.preprints.org) | NOT PEER-REVIEWED | Posted: 22 June 2023 doi:10.20944/preprints202306.1610.v1

The solid mixtures obtained by spray-drying (*Protocol 1*) were analyzed by DSC at 5K/min heating rate. Figure 11 (a) shows the profiles versus composition on heating. Figure 11 (b) collects the onset and endset of melting peak (solid filled circles). The resulting binary system includes a solidus and a liquidus which are rather flat up to 60wt.% $NaBrO_3$. This seems consistent with the tie-lines of the ternary system at 25°C determined by Swenson and Ricci [6]. The binary system is consistent with a continuous solid solution by means of substitution.

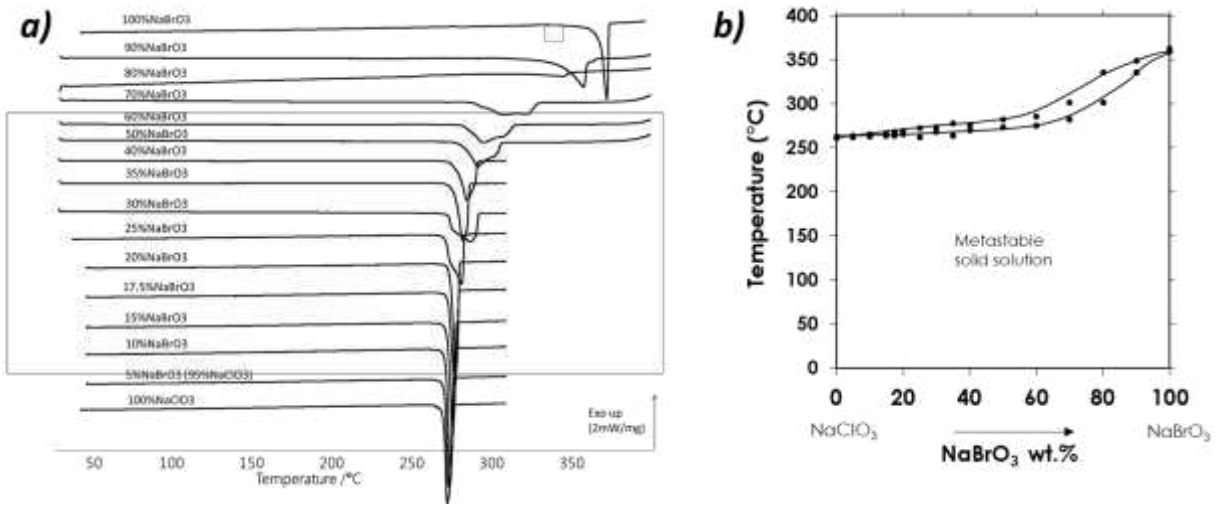

Figure 11. (a) DSC analyses (heating rate 5K.min^{-1}) of powder samples prepared by spray-drying (Protocol 1). (b) Racemic binary section of the quaternary system: $(NaClO_3)_L/(NaClO_3)_D/(NaBrO_3)_L/(NaBrO_3)_D$. for which a metastable solid solution could be obtained.

In order to increase the productivity of spray-drying, a mixture of 50% (mass) was used with protocol 2 (concentration 8 times higher than with protocol 1 and the temperature of the feeding liquid was 60°C). With these new parameters, part of the solid was stuck on the upper part of the drying chamber. The rest was stuck on the outlet of the drying chamber or in the collector bowl.

XRPD analyses of the solid in the drying chamber and the collector bowl are displayed in Figure 12 (The solid stuck at the outlet of the drying chamber appeared identical to that in the collector bowl). The two XRPD patterns shows a clear difference: (i) the powder stuck in the upper part of the drying chamber is duplicated testifying the presence of two similar solid solutions (ii) the powder sampled from the collector bowl is a single phase with diffraction peaks having intermediate d-spacings in comparison with the two partial solid solutions. For the former the full and fast dehydration is aborted resulting in two solid solutions, for the latter a fast and completed dehydration leads to a unique solid solution with the same composition as the feeding solution. For this solid, this is the same result as when using protocol 1.

If the powder obtained after spray-drying in the collector bowl is put for one day under 84% relative humidity at RT, the single XRPD signature spits into two resembling XRPD patterns just like what is obtained by complete slow evaporation.

Preprints (www.preprints.org) | NOT PEER-REVIEWED | Posted: 22 June 2023 doi:10.20944/preprints202306.1610.v1

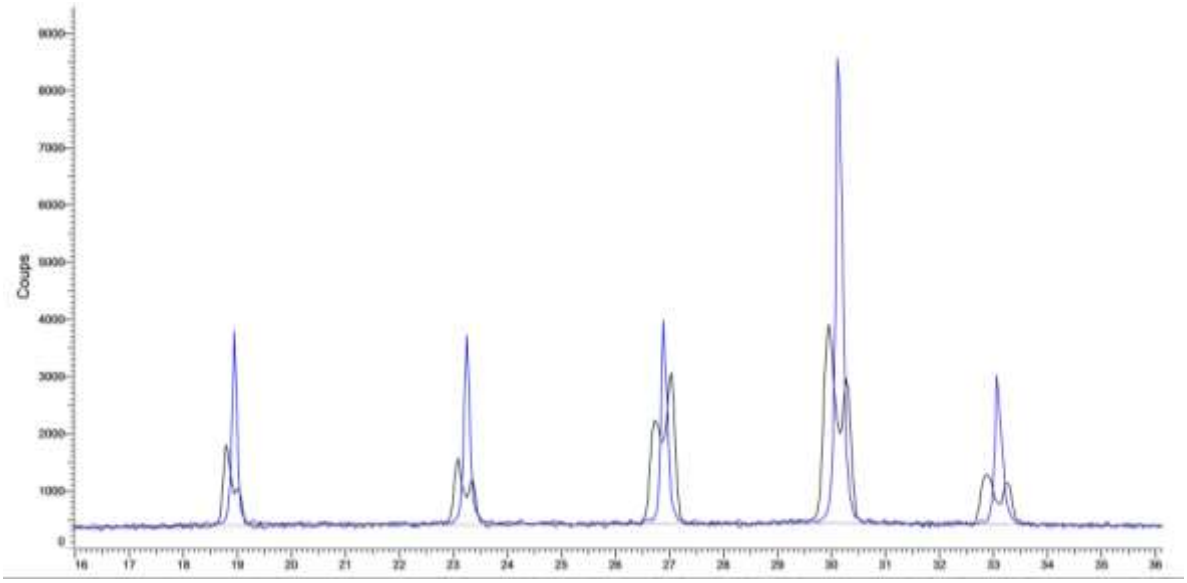

Figure 12. 50% mass after Spray drying protocol 2: (black pattern) solid collected in the upper part of the drying chamber; (blue pattern): solid from the collector bowl.

These results demonstrate that, whatever the composition, the two components could be forced to mix completely if the kinetics of crystallization is fast enough and if the drying is completed in a single step such as during spray-drying using protocol 1. Of course, under these conditions homochirality cannot be controlled; the final product is a random distribution of chiral particles -probably close to a racemic mixture. Thus, the binary section presented in Figure 11 (b) is merely a metastable racemic section of the quaternary system:

$NaClO_3$\\ - $NaClO_3$// - $NaBrO_3$\\ - $NaBrO_3$//, The symbols: \\ and// refer to opposite supramolecular chirality. The crystallographic features of the two components: same space group and a small difference only of the cubic parameter (less than 2% at RT) render possible the existence of two mirror image metastable complete solid solutions.

4. Conclusion & Perspectives

Spray-drying is a technique which favorizes access to metastable states because the entire crystallization -including nucleation, growth and complete drying- takes place in the order of one second. By using this energetic and swift process, the sodium chlorate and sodium bromate appear fully miscible from RT to fusion but the two-mirror-image complete solid solutions are actually, in a metastable state. Strangely enough, the metastable part of the solid solution corresponds to a slightly denser crystal lattice than the mean of the two stable limiting solid solutions. When the relative humidity exceeds a threshold ca. 75-84% the two (lefthanded and righthanded) complete solid solutions spit into mirror- image partial solid solutions.

For big particles such as those obtained by slow evaporation without stirring, this work evidences the presence of domains rich in bromate and others rich in chlorate which have epitaxial relationships. At 20°C, as a rough approximation, the composition range of NaClO3-rich solid solution is circa: 0%- 20% wt%, the composition range of NaBrO3-rich solid solution is circa 70%-100% wt%.

The construction of the genuine stable phase diagram does not appear that straightforward. Indeed, in addition to the formations of the partial solid solutions it is necessary to reach homochirality. This could be ensured by a continuous grinding (but the pollution by material snatched off from the beads could be an issue) or temperature cycling assisted or not by ultrasounds. The kinetics of the attainment of the 'true' equilibrium depends on the doses of those treatments (I.e. intensity versus time).

Future work will focus on deracemization ss$NaClO_3$ rich and ss ss$NaBrO_3$ rich up to their limits in compositions. It will also be interesting to test the deracemization inside the miscibility gap of these two partial solid solutions. Actually, is there an influence of the two ss$NaClO_3$ rich and ss$NaBrO_3$ rich in order to reach identical supramolecular chirality so: homo-homochirality or by contrast: hetero-homochirality?

Supplementary Materials:

Preprints (www.preprints.org) | NOT PEER-REVIEWED | Posted: 22 June 2023 doi:10.20944/preprints202306.1610.v1

Conflicts of Interest: The authors declare no conflict of interest and agreed on the last version of the manuscript.

Author Contributions: Conceptualization, Gerard Coquerel; Data curation, Sylvain Marinel; Investigation, SIMON Florent, Nicolas Couvrat, Christelle Bilot and Gerard Coquerel; Methodology, Gerard Coquerel; Resources, Sylvie Malo; Writing – original draft, SIMON Florent and Gerard Coquerel; Writing – review & editing, Gerard Coquerel.

Reference

1. Vegard, L. The constitution of the solid solution and the space filling of the atoms. *Zeitschrift für Phys.* **1921**, *5*, 17-26.
2. King, H.W. Qualitative size-factors for metallic solid solutions. *J. Mater. Sci.* **1966**, *1*, 79–90.
3. Denton, A.R.; Ashcroft, N.W. Vegard's law. *Phys. Rev. A*. **1991**, *43*, 3161–3164.
4. Chandrasekaran, K.S.; Monhanlal, S.K. The x-ray anomalous dispersion and optical rotation in the crystalline solid solution $NaClO_3$: $NaBrO_3$. *Pramana* **1976**, *7*, 152-159.
5. Subhadra, K.G.; Hussain, K.A. Melting Temperatures of $NaClO_3$-$NaBrO_3$ Mixed Crystals. *Cryst. Res. Technol.*, **1987**, *22*, *6*, 827-833.
6. Swenson, T.; Ricci, J.E. The Ternary Systems $KBrO_3$-$KClO_3$-H_2O at 25°C and $NaBrO_3$-$NaClO_3$-H_2O at 25 and 50°C. *J. Am. Chem. Soc.* **1939**, *61*, 1974-1977.
7. Crundwell, G.Y.; Gopalan, P.; Bakulin, A.; Peterson; M.L.; Kahr, B. Effect of Habit Modification on Optical and X-ray Structures of Sodium Halate Mixed Crystals: The Etiology of Anomalous Double Refraction, *Acta Cryst.* **1997**, *B53*, 189–202
8. Dickinson, R.G.; Goodhue, E.A. The Crystal Structure of Sodium Chlorate and Sodium Bromate. *J. Am. Chem. Soc.* **1921**, *43(9)*, 2045-2055.
9. Abrahams, S.C.; Bernstein, J.L. Remeasurement of Optically Active $NaClO_3$ and $NaBrO_3$. *Acta Cryst.* **1977**, *B33*, 3601–3604.
10. Savage, A.; Miller, R.C. Measurements of Second Harmonic Generation of Ruby Laser Line in Piezoelectric Crystals. *Appl. Opt.* **1962**, 1, 661–664.
11. Simon, H.J.; Bloembergen, N. Second-Harmonic Light Generation in Crystals with Natural Optical Activity. *Phys. Rev.* **1968**, 171, 1104–1114.
12. Matsuura, T.; Koshima, H. Review : Introduction to chiral crystallization of achiral compounds. Spontaneous generation of chirality. *J. Photochem. Photobiol.* **2005**, *6*, 7-24.
13. Ramachandran, G.N.; Chandrasekaran, K.S. The Absolute Configuration of Sodium Chlorate. *Acta Crystallogr.* **1957**, *10*, 671–675.
14. Beurkskens-Kerssen, G.; Kroon, J.; Endeman, H.J.; Van Laar, J.; Bijvoet, J.M. Absolute Configuration and Rotatory Power of the Crystals of NaBrO3 and NaClO3, In *Crystallography and Crystal Perfection*, ed. Ramachandran, G.N. London Academic Press. **1963**, pp. 225-236,
15. Chandrasekhar, S.; Madhava, M.S. Optical roratory dispersion of crystals of sodium chlorate and sodium bromate. *Acta Cryst.* **1967**, *23*, 911.
16. Kipping, F.S.; Pope, W.J. Enantiomorphism. *J. Chem. Soc. Trans.* **1898**, *73*, 606–617.
17. Kondepudi, D.K.; Kaufman, R.J.; Singh, N. Chiral symmetry breaking in sodium chlorate crystallization, *Science*, **1990**, 250.
18. Kondepudi, D. K.; Prigogine, I. Sensitivity of nonequilibrium systems. *Phys. A Stat. Mech. Appl.* **1981**, *107*, 1–24.
19. Kondepudi, D.K.; Nelson, G.W. Chiral symmetry breaking in nonequilibrium systems. *Phys. Rev. Lett.* **1983**, *50*, 1023–1026.
20. Kondepudi, D.K.; Nelson, G.W. Weak neutral currents and the origin of biomolecular chirality. *Nature*. **1985**, *314*, 438–441.
21. Buhse, T.; Durand, D.; Kondepudi, D.; Laudadio, J.; Spilker, S. Chiral symmetry breaking in crystallization: the role of convection. *Phys. Rev. Lett.* **2000**, *84*, 4405–4408.
22. Viedma, C. Chiral symmetry breaking during crystallization: complete chiral purity induced by nonlinear autocatalysis and recycling. *Phys. Rev. Lett.* **2005**, *94(6)*, 065504.
23. Suwannasang, K.; Flood, A.; Rougeot, C.; Coquerel, G. Using Programmed Heating-Cooling with Racemization in Solution for Complete Symmetry Breaking of a Conglomerate Forming System; *Cryst. Growth Des.* **2013**, *13*, 3498-3504.
24. Rougeot, C.; Guillen F.; Plaquevent, J-C.; Coquerel; G. Ultrasound-Enhanced Deracemization: Towards the Existence of Agonist Effects in the Interpretation of Spontaneous Symmetry Breaking. *Cryst. Growth Des.* **2015**, *15*, 2151-2155.
25. Viedma, C.; Cintas, P. Homochiraliry beyond grinding: deracemizing chrial crystals by temperature gradient under boiling. *Chem. Commun*. **2011**, 47, 12786–12788.
26. Viedma, C.; McBride, J.M.; Kahr, B.; Cintas, P. Enantiomeric-Specific Oriented Attachment: Formation of Macroscopic Homochiral Crystal Aggregates from a Racemic System. *Angew. Chem. Int. Ed.* **2013**, 52, 10545–10548.
27. Schindler, M.; Brandel, C.; Kim, W.-S.; Coquerel, G. Temperature Cycling Induced Deracemization of $NaClO_3$ under the Influence of $Na_2S_2O_6$. *Cryst. Growth Des.* **2020**, *20*, 1, 414-421.
28. Akizuki, M.; Hampar, M.S.; Zusman, J. An explanation of anomalous optical properties of topaz. *Mineral. Mag.* **1979**, *43*, 237-241.
29. Akizuki, M. Crystal symmetry and order-disorder structure of brewsterite. *Am. Mineral.* **1987**, *72*, 645-648.
30. Akikuzi, M.; Konno, H. Internal texture and abnormal optical property of apophyllite. *N. Jahrb. Mineral. Abh.* **1985**, *151*, 99-115.
31. McBride, J.M.; Bertmann, S.B. Using Crystal Birefringence to Study Molecular Recognition, *Angew. Chem.* **1989**, *28*, 330-333.

Preprints (www.preprints.org) | NOT PEER-REVIEWED | Posted: 22 June 2023 doi:10.20944/preprints202306.1610.v1

32. Weisinger-Lewin, Y.; Frolow, F.; McMullan, R.K.; Koetzle, T.F.; Lahav, M.; Leiserowitz, L. Reduction of crystal symmetry of a solid solution: a neutron diffraction study at 15K and the host/guest system asparagine/aspartic acid. *J. Am. Chem. Soc.* **1989**, 111, 1035–1040.
33. Weissbuch, I.; Lahav, M.; Leiserowitz, L.; Meredith, G.R.; Vanherzeele, H. Centrosymmetric crystals as host matrices for second-order optical nonlinear effect. *Chem. Mater.* **1989**, 1, 114–118.
34. Shimon, L.J.W.; Vaida, M.; Frolow, F.; Lahav, M.; Leiserowitz, L.; Weissinger-Lewin, Y.; McMullan, R.K. Symmetry lowering in crystalline solid solutions: a study of cinnamamide-thienylacrylamide by X-ray and neutron diffraction and solid state photochemistry. *Faraday Discuss.* **1993**, 95, 307.
35. Kahr, B.; McBride, J.M. Optically Anomalous Crystals. *Angew. Chem. Int. Ed. Engl.* **1992**, *31*, 1-26.
36. Kahr, B.; Gurney, R.W. Dyeing crystals. *Chem. Rev.* **2001**, *101*, 893–951.
37. Buckley, H. E. 2. The Influence of RO_4 and Related Ions on the Crystalline Form of Sodium Chlorate. *Zeitschrift für Krist.* **1930**, 15–31.
38. Ristic, R.; Sherwood, J.N.; Wojciechowskf, K. Morphology and growth kinetics of large sodium chlorate crystals grown in the presence and absence of dithionate impurity. *J. Phys. Chem.* **1993**, *97*, 10774–10782.
39. Ristic, R.; Shekunov, B.Y.; Sherwood, J.N., Growth of the tetrahedral faces of sodium chlorate crystals in the presence of dithionate impurity. *J. Cryst. Growth.* **1994**, *139*, 336–343.
40. Lan, Z.-P.; Lai, X.; Roberts, K.; Klapper, H. X-ray Topographic and Polarized Optical Microscopy Studies of Inversion Twinning in Sodium Chlorate Crystals Grown in the Presence of Sodium Dithionate Impurities, *Cryst. Growth Des*. **2014**, *14*, 6084–6092
41. Gopalan, P.; Peterson, M.L.; Crundwell, G.; Kahr, B. Reevaluating Structures for Mixed Crystals of Simple Isomorphous Salts: $NaCl_xBr_{1-x}O_3$. *J. Am. Chem. Soc.* **1993**, *115*, 3366–3367
42. Kaminsky, W.; Claborn, K.; Kahr, B.; *Chem. Soc. Rev.* Polarimetric imaging of crystals, **2004**, *33*, 514-525.
43. Sanjeevi Raja, C.; Mohanlal, S.K.; Chandrasekaran, K.S. An X-ray diffraction study of the size effect on a crystalline solid solution of sodium halates. *Zeitschrift für Krist.* **1984**, *166*, 121-127.
44. Shtukenberg, A.G.; Rozhdestvenskaya, I.V.; Popov, D.Y.; Punin, Y.O. Kinetic ordering of atoms in sodium chlorate-bromate solid solutions. *J. Solid State Chem.* **2004**, *177*, 4732–4742
45. Su, J.; Song, Y.; Zhang, D.; Chang, X. Characterization of unidirectionally grown $NaCl_{1-x}Br_xO3$ crystals. *Powder Diffr.* **2009**, *24*, 234–238.
46. Hulliger, J.; Wüst, T.; Brahimi, K.; Burgener, M.; Aboufadl, H. A stochastic principle behind polar properties of condensed molecular matter. *New J. Chem.* **2013**, *37*, 2229-2235.
47. Coquerel, G.; Sanselme, M.; Lafontaine, A.; Method and Measuring Scattering of X-Rays, Its Applications and Implementation Device, US Patent 9,955,898. **2016**.
48. Bak, S.Y.; Coquerel, G.; Kim, W.-S.; Park, B.J.; Solution Volume Effects on Spontaneous Chiral Symmetry Breaking of Sodium Chlorate Crystals; *J. Phys. Chem. Lett.* **2023**, *14*, 785-790.